

## Numerical Analysis of Tubular XT Joint of Jacket Type Offshore Structures under Static Loading

Md. Jobayer Mia<sup>1\*</sup>, Md. Abidul Islam<sup>2</sup>, Asif Kabir<sup>3</sup> and Mehran Islam<sup>4</sup>

### *Abstract*

*Jacket structures are made of welded tubular space frames supported by a lateral bracing system. Tubular members are made up of structural steel. In an offshore structure, their primary job is to resist yield and buckling loads. They are also used to resist lateral loads. There are various types of tubular joints like T, K, KT, XT, etc. and each of the joints has significance, depending on the structure design and environment. These joints are subjected to various types of cyclic loading. As a result, fatigue failure occurs with the passing of time. In this study, the Finite Element Model of the XT-type tubular joint has been created and analysis has been done under static loading by using the STATIC STRUCTURAL analysis system of ANSYS 19.2 commercial software. The XT tubular model was analyzed under different load cases, and corresponding values for stress, strain, and deformation were tabulated. Using the maximum stress value, the yield point of the joint was also determined. The results highlighted that as the thickness of the joint increases, the values of maximum stress, strain, and deformation decrease. It was also observed that for tensile and compressive loading, the joint yielded at 30 KN of loading.*

**Keywords:** Tubular joint, XT joint, Jacket structures, Chord, Brace, Static strength analysis.

### **1. Introduction**

The jacket is one of the most important structural components to establish an offshore structure in the marine environment. It is installed to sustain the decks of the structure

---

<sup>1</sup> Department of Naval Architecture and Offshore Engineering, Bangabandhu Sheikh Mujibur Rahman Maritime University, Dhaka, Bangladesh.

<sup>2</sup> Department of Naval Architecture and Offshore Engineering, Bangabandhu Sheikh Mujibur Rahman Maritime University, Dhaka, Bangladesh.

<sup>3</sup> Department of Mechanical Engineering, Bangladesh University of Engineering and Technology (BUET), Dhaka, Bangladesh

<sup>4</sup> Department of Naval Architecture and Offshore Engineering, Bangabandhu Sheikh Mujibur Rahman Maritime University, Dhaka, Bangladesh

\*Corresponding Author

naoe17002.jobayer@bsmrmu.edu.bd

under various loads. The factor of safety is an essential calculation, and it is calculated before designing the jacket. It assures that, the jacket can sustain in extreme weather conditions. The jackets are made of tubular sections, and the sections are made of anti-corrosive materials. These sections are connected by joints around the structure. There are many types of tubular joints available, such as T joint, K joint, Y joint, KT joint, XT joint, DT joint, X joint, DKDT joint, DYDT joint, DT joint, etc. An illustration of different tubular joints is presented in figure 1.

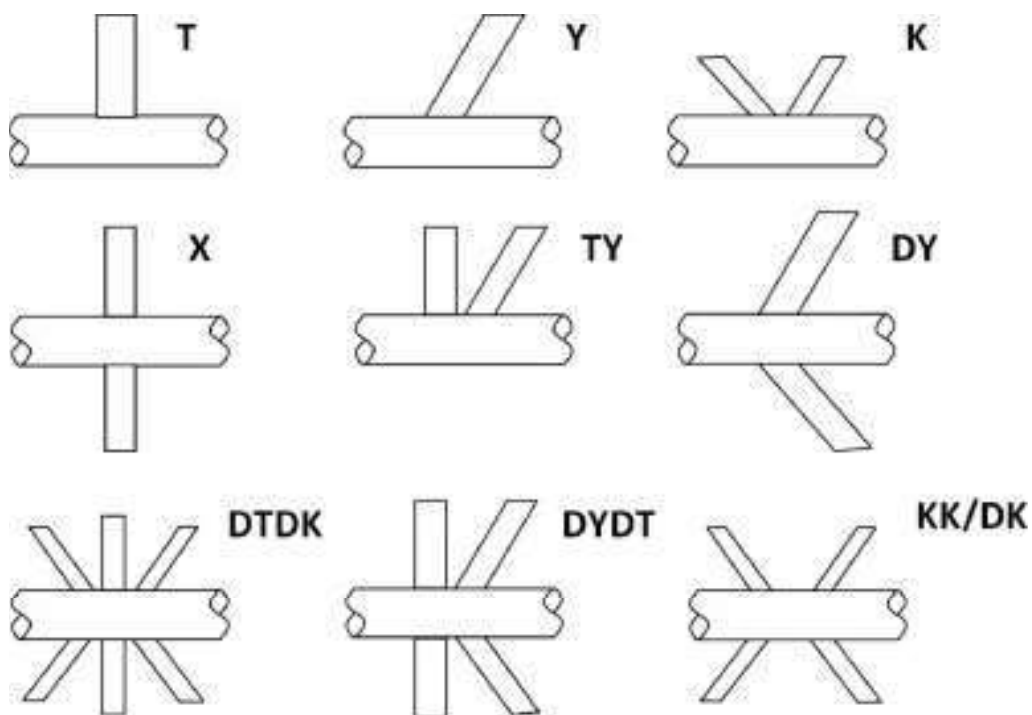


Figure 1: Types of tubular joints (Saini et al. 2016).

A tubular joint has two primary parts. One is called the chord that has the largest diameter, and the other part is known as the brace. The classification of the tubular joints is not only entirely determined by the geometry but also by the axial loads of different members. Tubular joints are designed to resist various types of loads. Such as wave load, marine growth loading, etc. The loads also vary with the marine environment. The service or longevity of a jacket structure significantly depends on the members, joints, etc. These loading conditions can easily cause a joint failure that might lead to a breakdown of the offshore structure. Therefore, the analysis is a must before designing the jacket, so it can resist the loads even in extreme conditions.

In this study, an XT-type tubular joint has been modeled and numerical analysis has been performed using the Finite Element Method (FEM). The XT tubular joint has one chord and two braces (reference brace and carryover brace). A typical XT tubular joint has been presented in figure 2.

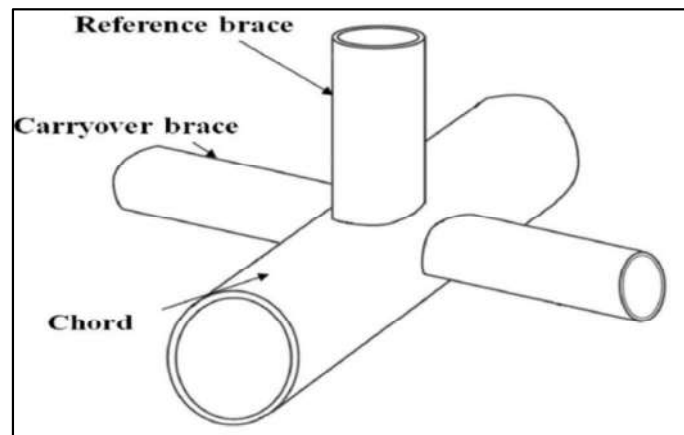


Figure 2: Illustration of tubular XT joint (Saini et al. 2016).

Axial loading (tensile and compressive) and bending moment were applied in the model to calculate the corresponding maximum stress, strain, and deformation values. The results of this study will highlight the features of the XT joint and may help the structure's designers work to increase the lifespan of the structure.

## 2. Literature Review

Offshore structures are installed on the seabed for the exploration of oil and gas from the sea bottom. Tubular joints are widely used as a primary construction element. These joints resist various types of loads to provide stability to the structure. Otherwise, it is naturally tougher to work in the marine environment. Many researchers and experts are working on these joints to make them more sustainable for decades. Aaghaakouchak and Dharmavasan (1990), Ramachandra et al. (1992), and Nwosu et al. (1995) worked with various types of tubular joints and their behavior on different loads. Researchers tried to find errors in their respective joint designs and compared the model analysis with experimental data to make further improvements for the real-life structure. Similar kinds of work can be found on Mayers et al. (2001) and Hoon et al. (2001) with different load conditions. Santosh Sawant and Muthumani (2020) worked on the K joint and KT joint have shown a comparative analysis over the same loading condition. Bittencourt et al. (2007) also worked on the K joint under static loading and compared

the numerical results to the experimental results. The same approaches were also used by Cao et al. (1998), Packer et al. (1993), Choo et al. (2003), and Koseteski et al. (2003) to analyze the K and KT joints. There is a pile of work on the T joint as well. Satyanarayana et al. (2011) analyzed T joint and compared the results with experimental results. Hamed et al. (2001) performed an analysis on elliptical T-tubular joints and compared the result with circular chord tubular joints. The analysis was performed through finite element analysis or the finite element method. Murthy (2002) worked on unstiffened T-joints. He estimated the strength of the joint under axial compression load. Cofer and Will (1992) developed a non-linear finite element computer program to model welded tubular T joints and DT joints. Many researchers thought about theoretical approaches to describing tubular joints. Beale and Toprac (1967) analyzed T, Y, and K joints using theoretical formulae.

There is also a large amount of work-based deflection criteria. Deflection criteria are directly related to stress-strain values. Lu et al (1994) proposed a limit for the deformation. Later, Choo et al. (2003) used that deformation limit to evaluate the axial and rotational capacity of a joint subjected to the corresponding brace axial or moment loads. Moreover, the Stress Concentration Factor (SCF) is a vital subject for numerical analysis of tubular joints. It helps to understand stress-strain characteristics in detail. Ahmadi et al. (2012) Ahmadi and Yaghin (2012), Dallyn et al. (2015) have a diverse body of work in SCF-related studies. Cheiw et al. (1999) and Ahmadi and Kouhi (2020) analyzed XT joints and displayed their important findings.

The analysis of the XT joint is shown in the current study. The type of analysis shown in this paper can be found in Chandran and Arathi's (2016) work on K joint. The features of tubular joints under tensile and compressive loading, as well as bending moment, will be numerically analyzed in this work. The efficiency and applicability of XT tubular joints in jacket-type offshore structures will also be investigated in the present study.

### **3. Methodology**

In this study, the Finite Element Method (FEM) was used to analyze the XT tubular joint. FEM was used because it is difficult to use closed-form solutions for determining stress and strain in tubular structures due to the complex geometry of the joints (Sadat Hosseini et al. 2018). For the current study, numerical analysis of the model has been performed by following the steps shown in figure 3.

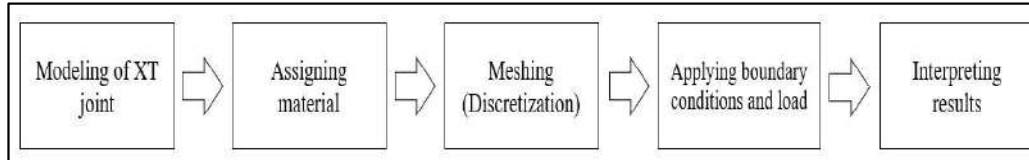


Figure 3: Steps of the model analysis.

### 3.1 Governing equations

Stress ( $\sigma$ ) is the measurement of applied forces per unit area at a point of a solid body. The stress field is expressed in vector form  $\sigma = \{\sigma(x, y, z)\}$  as-

$$\sigma = [\sigma_x, \sigma_y, \sigma_z, \tau_{yz}, \tau_{zx}, \tau_{xy}]^T \dots (1)$$

Where  $\sigma_x, \sigma_y, \sigma_z$  are normal stresses and  $\tau_{yz}, \tau_{zx}, \tau_{xy}$  are shear stresses. Von Mises stress is used as a criterion for determining the onset of failure in materials (Chandrupatla and Belegundu 2009). The Von Mises stress  $\sigma_{VM}$  is given by-

$$\sigma_{VM} = \sqrt{I_1^2 - 3I_2} \dots (2)$$

Where  $I_1$  and  $I_2$  are the first two invariants of the stress tensor. For the general state of stress,  $I_1$  and  $I_2$  are given by

$$I_1 = \sigma_x + \sigma_y + \sigma_z$$

$$I_2 = \sigma_x\sigma_y + \sigma_y\sigma_z + \sigma_z\sigma_x - \tau_{yz}^2 - \tau_{xz}^2 - \tau_{xy}^2 \dots (3)$$

“Strain ( $\epsilon$ ) is the ratio of the change in length caused by the applied force, to the original length (Singer and Pytel 1980)”. Strain in vector form is represented as

$$\epsilon = [\epsilon_x, \epsilon_y, \epsilon_z, \gamma_{yz}, \gamma_{zx}, \gamma_{xy}]^T \dots (4)$$

Where,  $\epsilon_x, \epsilon_y, \epsilon_z$  are normal strains and  $\gamma_{yz}, \gamma_{zx}, \gamma_{xy}$  are shear strains.

If the axial stress is applied in the x-direction, then strain is represented as (Budynas and Nisbett 2014)-

$$\epsilon_x = \frac{\sigma_x}{E} \dots (5)$$

Where E is the modulus of elasticity. For small deformation, the strain displacement relation is signified as (Chandrupatla and Belegundu 2009)-

$$\epsilon = \left[ \frac{\partial u}{\partial x}, \frac{\partial v}{\partial y}, \frac{\partial w}{\partial z}, \frac{\partial v}{\partial z} + \frac{\partial w}{\partial y}, \frac{\partial u}{\partial z} + \frac{\partial w}{\partial x}, \frac{\partial u}{\partial x} + \frac{\partial v}{\partial x} \right]^T$$

### 3.2 Numerical modeling

Numerical modeling for the current study was done by using ANSYS 19.2 software. The geometry of the XT tubular joint was created in the design modeler of the programming bundle of ANSYS named STATIC STRUCTURAL. The selection of dimensions depends on the pile sizes that are going to be installed in jacket-type offshore structures (Santosh Sawant and Muthumani 2020). For the current study, the dimension of the model has been chosen as the proposed model of Hamid et al. (2001) for determining suitable results. The dimension of different geometric parameters of the model is shown in table 1. The developed model for this study is shown in figure 4.

**Table 1:** Geometric dimension of XT joint.

Geometric Parameters	Chord	Brace
Diameter	76.2 mm	42.5 mm
Length	440 mm	200 mm
Thickness	2 mm	2 mm

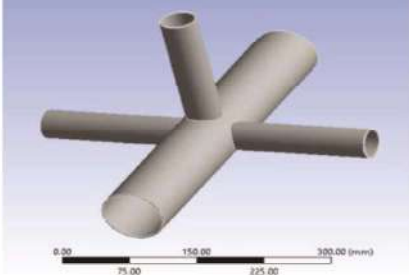


*Figure 4: Developed XT tubular joint model.*

Structural steel was used to model the geometry. Young's modulus and Poisson's ratio were chosen as  $2 \times 10^5$  MPa and 0.3, respectively. The material properties of the model are shown in table 2.

**Table 2:** Material specifications of the model.

Engineering Properties	Specifications
Material used	Structural steel
Density	$7850 \text{ kg/m}^3$
Young's Modulus	$2 \times 10^5 \text{ MPa}$
Poisson's Ratio	0.3
Bulk Modulus	$1.67 \times 10^{11} \text{ Pa}$
Shear Modulus	$7.69 \times 10^{10} \text{ Pa}$
Yield Stress	250 MPa

### 3.3 Meshing

Meshing is a phenomenon in which the entire geometry is divided into smaller elements to obtain correct results under specific loading situations (Lie et al. 2003). For this study, the meshing of geometry was done in the meshing module of the STATIC STRUCTURAL workbench. Customized element size type meshing was selected. To avoid numerical errors, an effort was made to design a regular mesh with the correct element size (Bittencourt et al. 2007). The default meshing size was 31.927 mm, but it was reset to 10 mm to have quality meshing. The model was divided into 20474 nodes and 10139 elements for the ease of simulation and getting good results. The physical preference for meshing was mechanical (Ahmadi and Masoud 2019). The generated mesh of the model is shown in figure 5.

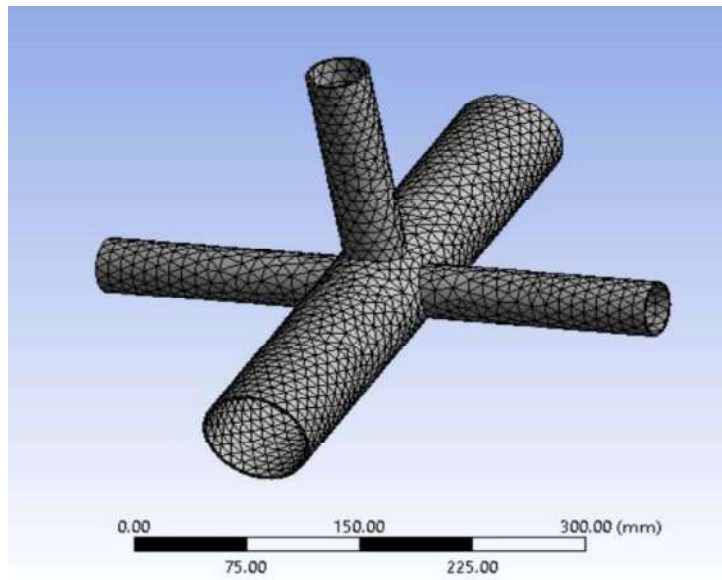


Figure 5: Generated mesh for the XT tubular joint model.

### 3.4 Boundary conditions and loading

In this study, boundary conditions were applied to the chord. As the ends of the chord are welded into jacket-type offshore structures. So, the ends of the chord were kept fixed for all degrees of freedom. Three types of loading such as tension, compression, and bending moment were applied during this study. For tension and compression, the force is distributed equally to each of the free ends of the braces where the upward direction of loading indicates tension and the downward direction of loading indicates

compression. Both tensile and compressive loading were applied as remote forces in the ANSYS simulation module so that the forces could be distributed uniformly along with the braces (Chandran and Arathi 2016). The bending moment was also applied at the end of the braces. While applying bending moment, a couple formed and the net direction was perpendicular to the chord. Loads and moments were applied gradually so that the corresponding stress, deformation, and strain values could be obtained evidently. The boundary conditions and loading are shown in figure 6.

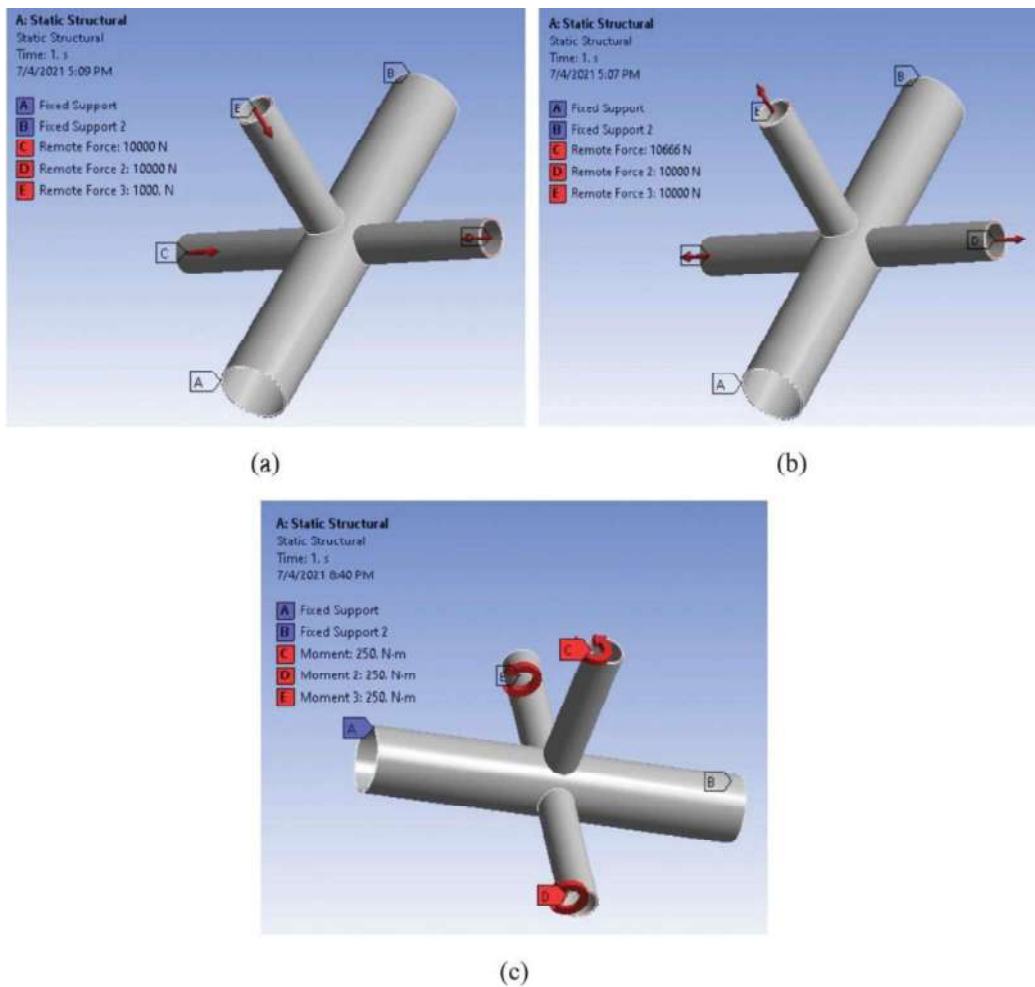


Figure 6: Illustration of boundary conditions and applied (a) a compressive force, (b) tensile force, and (c) bending moment.



#### 4. Results and Discussion

After completing the analysis in the ANSYS workbench, the maximum values of stress, strain, and deformation have been found for different load cases and have been described in this section. These results are demonstrated by using tables, graphs, and visual representations.

##### 4.1 Load cases and yielding points of the model

The yield point is defined as the point where the material deforms a larger amount with a small increase in loading. After this point, the plastic region of the material starts. Three types of loads (compression, tension, and bending moment) were applied separately in the model and for each case, the loading was increased gradually, and analysis was done to obtain the yield point of the model.

The yielding point of the model was found at 30 KN for axial compression and tension. And, for the bending moment, the yield point was found at 0.74 KNm of the applied moment. Table 3 shows yielding points for all the load cases.

**Table 3:** Load cases and yielding points of the model.

Load type	Yielding point
Compression (KN)	30
Tension (KN)	30
Bending moment (KNm)	0.74

##### 4.2 Relation of maximum stress, strain, and deformation with chord thickness

For both tension and compression, chord thickness and loads have been increased gradually. As a result, maximum stress decreased with higher chord thickness, and the yielding point was found in the larger load value. Representation of the equivalent stress, strain, and deformation distribution of the model under axial forces is demonstrated in Figure 7.

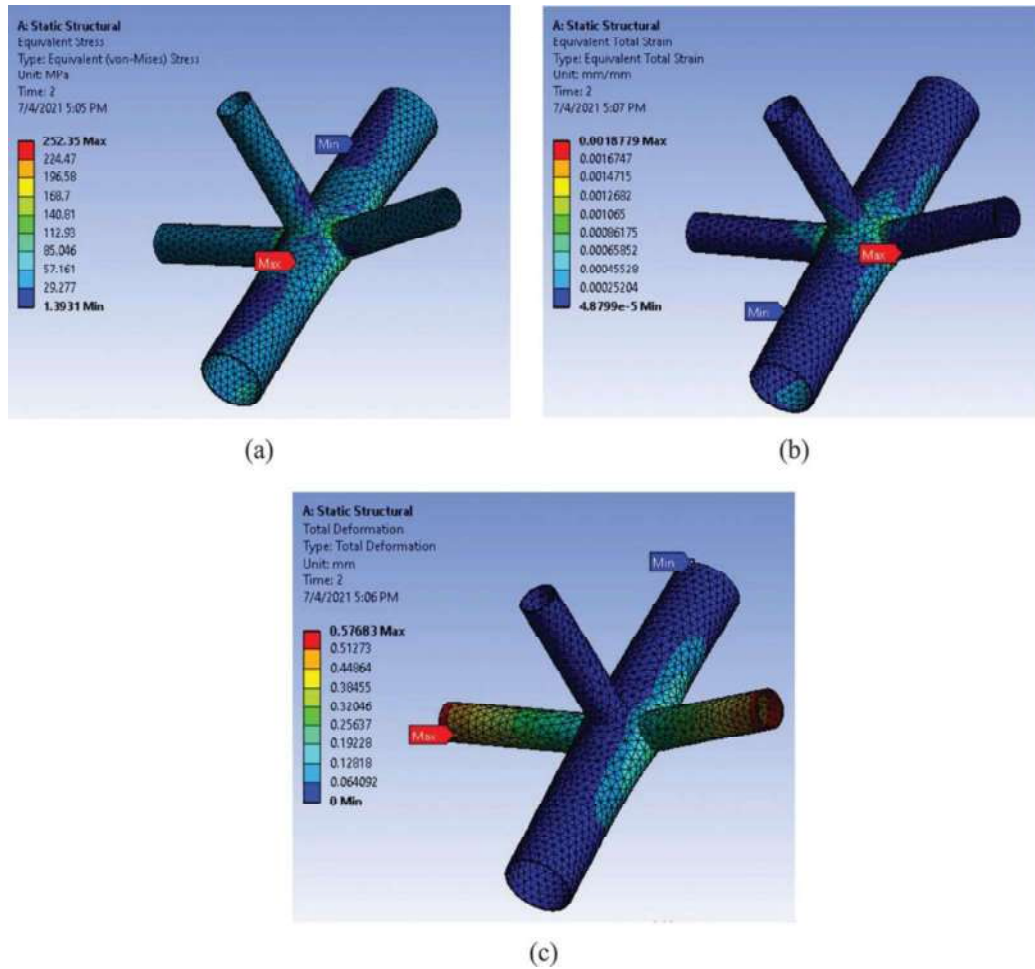


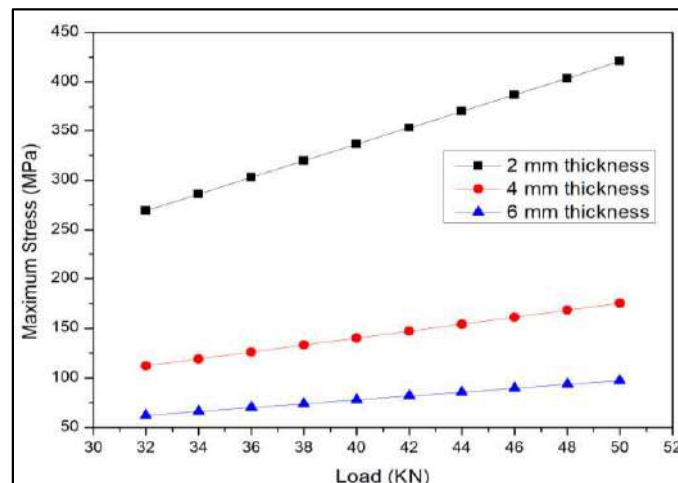
Figure 7: Representation of equivalent (a) stress, (b) strain, and (c) deformation distribution of model under axial forces.

Table 4 is showing how the maximum stress is changing with load and chord thickness. It defines that a joint can stand without any fracture even in a higher amount of load when the thickness rises.

**Table 4:** Maximum stress values for different loads varying thickness.

Load (KN)	Maximum stress (MPa)		
	2 mm	4 mm	6 mm
32	269.16	112.04	62.28
34	285.99	119.05	66.18
36	302.82	126.06	70.11
38	319.63	133.07	74.01
40	336.46	140.08	77.90
42	353.29	147.09	81.80
44	370.30	154.10	85.69
46	386.93	161.11	89.59
48	403.74	168.12	93.48
50	420.57	175.11	97.38

It is found from table 4 that the maximum stress is 269.16 MPa when the load is 32 KN and the chord thickness is 2 mm. But the stress reduced by 58.37% under the same load just after increasing the thickness by 2mm, and it became 112.04 MPa only. It reduced by 44.12% more when the thickness becomes 6 mm. At the bottom, the stresses are 420.57, 175.11, 97.38 MPa under 50 KN axial loads with the thickness of 2, 4, 6 mm respectively. So, the maximum stress has a proportional relationship with the loads, but a disproportional relationship with the chord thickness. In both ways, a linear graph is found and it has been shown in Figure 8. The graph shows a huge decrease of stress when thickness increases from 2mm to 4 mm, but a slight decrease of stress when thickness increases to 6 mm from 4 mm.



*Figure 8: Variations in maximum stress for different thicknesses.*

Primarily, a material deforms due to applied forces (internally or externally). There are two types of deformation, elastic and plastic. When the joint is unable to handle the load, it fractures. Table 5 shows the change of maximum deformation under increasing load and thickness. Maximum deformation increases if the axial load is increased, which indicates a proportional relation, but deformation decreases if the thickness is increased. The deformation is 0.61 mm under 32 KN load with 2 mm thickness. And deformation increases with higher loads on the same thickness, it becomes 0.96 mm under 50 KN loads.

Again, for 34 KN load, the deformation is found at 0.16 mm and 0.08 mm with 4 mm and 6 mm of thickness respectively. This disproportional relation is true for every case. Table 5: Maximum deformation values for different loads varying thickness.

Load (KN)	Maximum deformation (mm)		
	2 mm	4 mm	6 mm
32	0.61524	0.16396	0.08120
34	0.65372	0.17421	0.08630
36	0.69219	0.18446	0.09180
38	0.73061	0.19471	0.09690
40	0.76908	0.20496	0.10200
42	0.80756	0.21521	0.10710
44	0.84604	0.22546	0.11220
46	0.88452	0.23571	0.11730
48	0.92301	0.24596	0.12240
50	0.96148	0.25619	0.12750

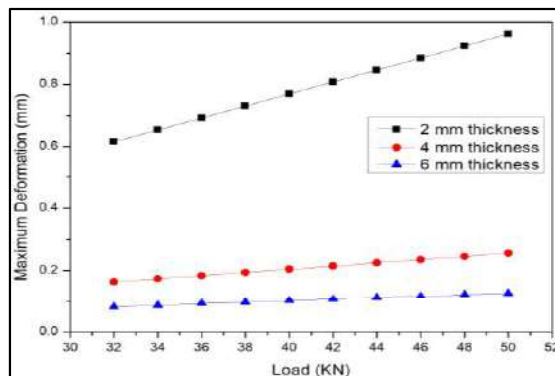


Figure 9: Variations in maximum deformation for different thicknesses.

Figure 9 shows the graphical representation of changing deformation under various loads and thicknesses. The deformation drops significantly when the thickness is increased from 2 to 4 mm. But when the thickness is increased from 4 to 6 mm, deformation drops slightly.

Earlier, the deformation had been explained. The quantity that can describe deformation is known as strain. Strain is a ratio between the amount of deformation experienced by the body in the direction of force applied and the initial dimensions of the body. Table 6 describes the change of strain under increasing load with increasing thickness.

It is found that the strain increases when the load increases, but it decreases when the thickness decreases. Maximum strain is found at 0.002 mm when the load is 32 KN and the thickness is 2 mm. But it becomes 0.0007 mm and 0.0003 mm under the same load with 4- and 6-mm thickness respectively. The same pattern goes with other loads as well.

**Table 6:** Maximum strain values for different loads varying thickness.

Load (KN)	Maximum strain (mm/mm)		
	2 mm	4 mm	6 mm
32	0.002003	0.000721	0.000350
34	0.002128	0.000766	0.000370
36	0.002254	0.000811	0.000396
38	0.002379	0.000856	0.000418
40	0.002504	0.000901	0.000440
42	0.002629	0.000946	0.000462
44	0.002754	0.000991	0.000484
46	0.002880	0.001037	0.000506
48	0.003005	0.001082	0.000528
50	0.003130	0.001127	0.000550

Figure 10 shows the graphical view of the findings from Table 6. Maximum strain goes down dramatically when the thickness is increased from 2 to 4 mm, but when the thickness reaches 6 mm, the strain value drops slightly.

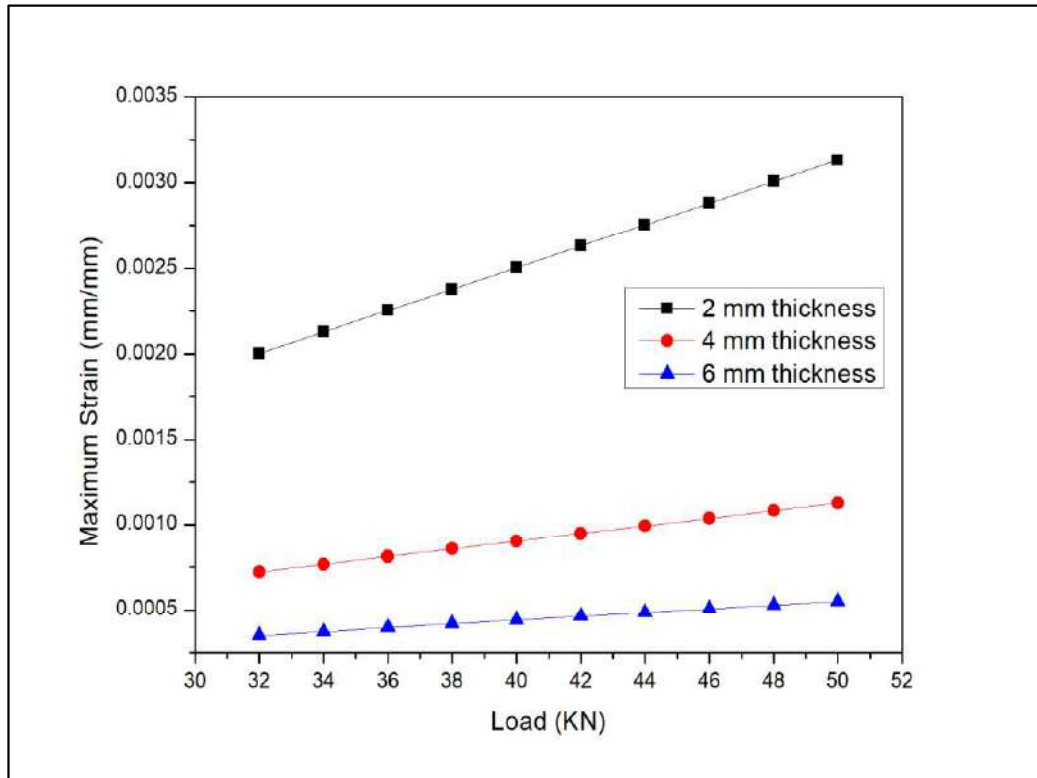


Figure 10: Variations in maximum strain for different thicknesses

### 4.3 Bending Moment

The bending moment is the third type of load, which is the internal reaction to a bending load that has been used here to analyze the tubular XT joint. It acts on a surface that is normal to the neutral axis. Figure 11 shows the equivalent stress, total deformation, and equivalent strain distribution caused by the bending moment of the tubular XT joint.

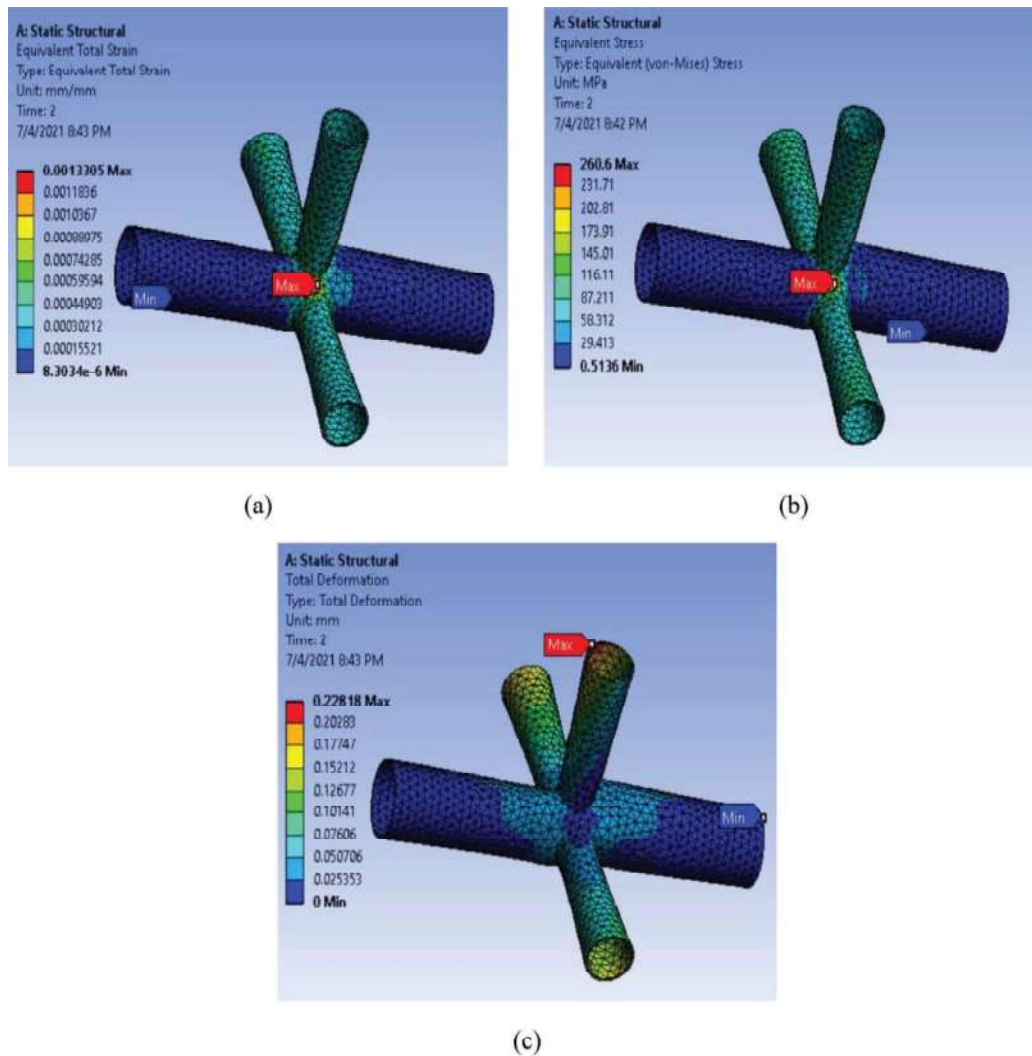


Figure 11: Representation of (a) equivalent stress, (b) total deformation, and (c) equivalent strain distribution of model under bending moment.

Table 7 describes the relationship between stress, deformation, and strain with bending moment (BM). All three have a proportional relationship with BM. Stress, deformation, and strain. All three increase when BM increases. Maximum stress is 260.06 Mpa when BM is 0.75, and it reaches 343.95 Mpa when BM is 1. The other two increase in the same manner.

**Table 7:** Maximum stress, deformation, and strain values for different bending moments.

BM (KNm)	Maximum Stress (MPa)	Maximum deformation (mm)	Maximum strain (mm/mm)
0.75	260.06	0.22818	0.0013305
0.78	271.03	0.23731	0.0013837
0.81	281.45	0.24643	0.0014369
0.84	291.87	0.25555	0.0014901
0.87	302.29	0.26467	0.0015433
0.91	312.71	0.27379	0.0015965
0.94	323.13	0.28291	0.0016497
0.97	333.55	0.29203	0.0017029
1	343.95	0.30115	0.0017561

As it is mentioned that BM keeps a proportional relation with stress, deformation, and strain. So, it produces a linear graph. Figure 14 proves that with graphical view.

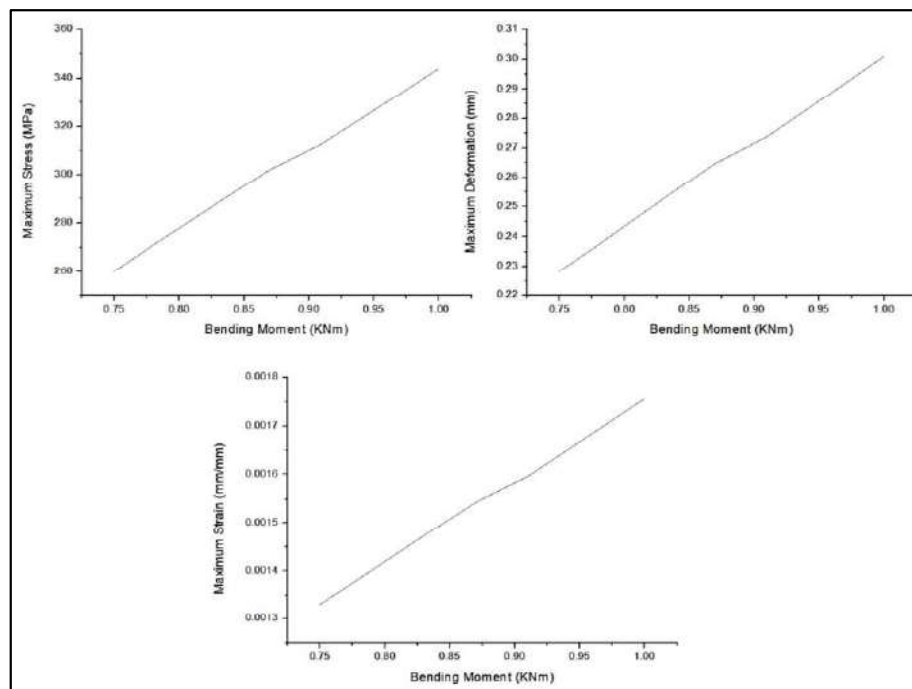


Figure 12: Illustration of maximum stress, deformation, and strain under bending moment.



## 5. Conclusion

The XT tubular joint is one of the most widely used joints in jacket-type offshore structures. The conclusion of this study can be drawn by summarizing the key findings from the numerical analysis of the tubular XT joint. The key findings can be summarized as follows:

1. For an equivalent stress distribution, maximum stress is found near the joint over the chord. Minimum stress is found between the joint and the top of the chord.
2. For total deformation distribution under axial load, maximum deformation is found on the top of a brace. On the other hand, the minimum deformation is found at the top edge of the chord.
3. For an equivalent strain distribution, maximum strain is found near the joint over a brace.
4. For the bending moment load case, maximum stress and deformation are found on the joint of the structure. Only maximum strain is found on the top of a brace.
5. The analysis shows that whenever thickness is increased from 2 mm to 4 mm; stress, strain, and deformation all drop by a significant amount. But when the thickness was increased again from 4 mm to 6 mm, all three parameters dropped slightly.
  - For axial load value, the stress decreases by 58.37% and 44.12% with an increase in thickness from 2 to 4 & 4 to 6 mm.
  - Again, for the deformation value, maximum deformation decreases by almost 50% when the thickness increases from 2 to 4 and 4 to 6mm.
  - Maximum strain decreases by 64% and almost 50% when the thickness increases from 2 to 4 mm, and 4 to 6 mm.
6. The tubular XT joint is more effective and performs better with the increase in thickness.

## References

Ahmadi, Hamid, and Ahmad Kouhi. 2020. "Stress Concentration Factors of Multi-Planar Tubular XT-Joints Subjected to out-of-Plane Bending Moments." *Applied Ocean Research* 96:102058. DOI: 10.1016/j.apor.2020.102058.

Ahmadi, Hamid, Mohammad Ali Lotfollahi-Yaghin, Shao Yong-Bo, and Mohammad H. Aminfar. 2012. "Parametric Study and Formulation of Outer-Brace Geometric Stress Concentration Factors in Internally Ring-Stiffened Tubular KT-Joints of Offshore Structures." *Applied Ocean Research* 38: 74–91. DOI: 10.1016/j.apor.2012.07.004.

Ahmadi, Hamid, and Mohammad Ali Lotfollahi-Yaghin. 2012. "A Probability Distribution Model for Stress Concentration Factors in Multi-Planar Tubular DKT-Joints of Steel Offshore Structures." *Applied Ocean Research* 34: 21–32. DOI: 10.1016/j.apor.2011.11.002.

Ahmadi, Hamid and Amini Niaki Masoud. 2019. "Effects of geometrical parameters on the degree of bending in two-planar tubular DT-joints of offshore jacket structures subjected to axial and bending loads." *Marine Structures* 64: 229–245. DOI: 10.1016/j.marstruc.2018.11.008

Aaghaakouchak, A. A. and S. Dharmavasan. 1990. "Stress analysis of unstiffened and stiffened tubular joints using an improved finite element model of intersection." *Proceedings of the Ninth International Conference on Offshore Mechanics and Arctic Engineering, Vol. III, Part A, Houston (TX), US, pp. 321-328.*

Bittencourt, M. C., L. R. O. de Lima, P. C. G. da S Vellasco., J. G. S. da Silva, and, L. F. da C. NevesA. 2007. "Numerical Analysis of Tubular Joints under Static Loading." *APCOM'07 in conjunction with EPMESC XI.*

Budynas, Richard G., and J. Keith Nisbett. 2014. *Shigley's Mechanical Engineering Design*. NY: McGraw-Hill Higher Education.

Beale, L.A and A.A. Toprac. 1967. "Analysis of T.Y.K. welded connections," *Bull structural steel committee*, Texas.

Chandran, Anju and Arathi S. 2016. "Static Strength Analysis of a Tubular K- Joint of an Offshore Jacket Structure." *International Journal of Science and Research (IJSR)* 5: 708-713.

Chandrupatla, Tirupathi R., and Ashok D. Belegundu. 2009. *Introduction to Finite Elements in Engineering*. Taipei: Pearson Education Taiwan Ltd.

Cao, J.J., J.A. Packer, and G.J. Yang. 1998. "Yield Line Analysis of RHS Connections with Axial Loads." *Journal of Constructional Steel Research* 48: 1–25. DOI: 10.1016/s0143-974x(98)90143-2.

Choo, Y.S., X.D. Qian, J.Y.R. Liew, and J. Wardenier. 2003. "Static Strength of Thick-Walled CHS X-Joints—Part I. New Approach in Strength Definition." *Journal of Constructional Steel Research* 59: 1201–28. DOI: 10.1016/s0143-974x(03)00054-3.

Cofer, William F., and Kenneth M. Will. 1992. "A finite element technique for the ultimate strength analysis of tubular joints." *Engineering Computations* 9: 345–58. DOI: 10.1108/eb023871.

Chiew, Sing-Ping, Chee-Kiong Soh, and Nai-Wen Wu. 1999. "Experimental and Numerical Stress Analyses of Tubular XT-Joint." *Journal of Structural Engineering* 125: 1239–48. DOI: 10.1061/(asce)0733-9445(1999)125:11(1239).

- Dallyn, Paul, Ashraf El-Hamalawi, Alessandro Palmeri, and Robert Knight. 2015. "Experimental Testing of Grouted Connections for Offshore Substructures: A Critical Review." *Structures* 3: 90–108. DOI: 10.1016/j.istruc.2015.03.005.
- Hamed, A F, Y A Khalid, B B Sahari, and M M Hamdan. 2001. "Finite Element and Experimental Analysis for the Effect of Elliptical Chord Shape on Tubular T-Joint Strength." *Proceedings of the Institution of Mechanical Engineers, Part E: Journal of Process Mechanical Engineering* 215: 123–31. DOI: 10.1243/0954408011530370.
- Hoon, Kay-Hiang, Looi-Kian Wong, and Ai-Kah Soh. 2001. "Experimental Investigation of a Doubler-Plate Reinforced Tubular T-Joint Subjected to Combined Loadings." *Journal of Constructional Steel Research* 57: 1015–39. DOI: 10.1016/s0143-974x(01)00023-2.
- Kosteski, N., J.A. Packer, and R.S. Puthli. 2003. "A Finite Element Method Based Yield Load Determination Procedure for Hollow Structural Section Connections." *Journal of Constructional Steel Research* 59: 453–71. DOI: 10.1016/s0143-974x(02)00066-4.
- Lu LH, de Winkel GD, Yu Y, Wardenier J. 1994. "Deformation limit for the ultimate strength of hollow section joints". *Proceedings of Sixth International Symposium on Tubular Structures*, Melbourne.
- Lie, S.T., C.K. Lee, and S.M. Wong. 2003. "Model and Mesh Generation of Cracked Tubular Y-Joints." *Engineering Fracture Mechanics* 70: 161–84. DOI: 10.1016/s0013-7944(02)00036-x.
- Myers, P.T., F.P. Brennan, and W.D. Dover. 2001. "The Effect of Rack/Rib Plate on the Stress Concentration Factors in Jack-up Chords." *Marine Structures* 14: 485–505. DOI: 10.1016/s0951-8339(00)00051-4.
- Murthy, J.S. Thandava. 2002. "Behavior of unstained Tubular joints." *Institute of Engineers Journal, Civil Engineering division*, 82: 224-228.
- Nwosu, D. I., A. S. Swamidas, and K. Munaswamy. 1995. "Numerical Stress Analysis of Internal Ring-Stiffened Tubular T-Joints." *Journal of Offshore Mechanics and Arctic Engineering* 117: 113–25. DOI: 10.1115/1.2827061.
- Packer, Jeffrey A. 1993. "Moment Connections between Rectangular Hollow Sections." *Journal of Constructional Steel Research* 25: 63–81. DOI: 10.1016/0143-974x(93)90052-t.
- Ramachandra Murthy, D. S., A. G. Madhava Rao, P. Gandhi, and P. K. Pant. 1992. "Structural Efficiency of Internally Ring-Stiffened Steel Tubular Joints." *Journal of Structural Engineering* 118: 3016–35. DOI: 10.1061/(asce)0733-9445(1992)118:11(3016).

Sadat Hosseini, Alireza, Mohammad Reza Bahaari, and Mohammad Lesani. 2018. "SCF Distribution in FRP-Strengthened Tubular T-joints under Brace Axial Loading." *Scientia Iranica* 27: 1113-1129. DOI:10.24200/sci.2018.5471.1293.

Santosh Sawant, Sanket, and K. Dr. Muthumani.2020. "Analysis of Tubular Joint of Offshore Structure." *Journal of Physics: Conference Series* 1716: 012012. DOI: 10.1088/1742-6596/1716/1/012012.

Singer, Ferdinand L., and Andrew Pytel. 1980. *Strength of Materials*. New York: Harper & Row.

Saini, Dikshant Singh, Debasis Karmakar, and Samit Ray-Chaudhuri. 2016. "A Review of Stress Concentration Factors in Tubular and Non-Tubular Joints for Design of Offshore Installations." *Journal of Ocean Engineering and Science* 1: 186–202. DOI: 10.1016/j.joes.2016.06.006.

Satyanarayana, K., R. T. Naik and L. V. Rao. 2011. "Static Strength Analysis of Tubular T-joints Using Ansys." *J. Basic. Appl. Sci. Res.* 1: 989-997.